Supporting information

The different time regions Δt_1, Δt_2, Δt_3 found by SAXS data analysis can be preliminarily distinguished upon inspection of the integrated intensity given by $\int_0^\infty I(q)dq$ as a function of time. We observe a different power law behavior in each of the three time ranges, as indicated by lines in Fig. 1; furthermore, we find the same power exponent 1.2 in the nucleation regions Δt_1 and Δt_3, and a different power exponent 3.9 in the growth region Δt_2.

The *log-normal* distribution *P(R)* of *particle size* used in Eq. 4, is defined by

$$P(R) = \frac{1}{Rs\sqrt{2\pi}} \exp -\frac{(\ln R - \rho)^2}{2s^2}, \text{ with } \int_0^\infty P(R)dR = 1 \qquad (1)$$

where ρ and s are the mean and the standard deviation values, respectively, of the distribution of the variable's natural logarithm; so, the mean and the standard deviation R_m and σ of the R distribution are given by

$$R_m = \exp\left(\rho + 12s^2\right) \text{ and } \sigma = R_m\left(e^{s^2} - 1\right). \qquad (2)$$

The interference term $S(q, R_{HS}, \eta)$ for a hard sphere model in monodisperse approximation was calculated with the Percus-Yevick equation:

$$S(q, R_{HS}, \eta) = \frac{1}{\left[1 + 24\eta A(2qR_{HS})\right]} \qquad (3)$$

with

$$A(x) = \int_0^1 y^2 (a + by + cy^3) \frac{\sin(yx)}{yx} dy \qquad (4)$$

and

$$a = \frac{(1+2\eta)^2}{(1-\eta)^4}; b = \frac{-6\eta(1+\eta 2)^2}{(1-\eta)^4}; c = \frac{a\eta}{2} \qquad (5)$$

R_{HS} and η are the hard sphere radius hard sphere volume fraction, respectively.

In Fig. 2 the reduced standard deviations (*rds*) $\Delta N/N$, $\Delta R_m/R_m$, $\Delta\sigma/\sigma$, $\Delta R_{HS}/R_{HS}$, $\Delta\eta/\eta$, $\Delta P_E/P_E$, $\Delta P_C/P_C$ of all estimated parameters are plotted as a function of the time. For $t<t_0$, $\Delta N/N$, $\Delta R_m/R_m$, $\Delta\sigma/\sigma$, $\Delta R_{HS}/R_{HS}$ and $\Delta\eta/\eta$ are quite large and assume values larger than 1 indicating that the model of Eq.2 cannot be applied to the analysis of the SAXS profiles before the addition of ascorbic acid. In this time range fitting procedure converges taking as a model the power law background $I_B(q)$; indeed, only $\Delta P_E/P_E$ and $\Delta P_C/P_C$ *rsd* assume small reasonable values as indicated in Fig. 2. As the reaction takes place, all the *rsd* reach the small value of 0.1 in the Δt_1 range and thus the model of Eq.2 takes to work in SAXS patterns analysis; in particular the fitting procedure converge when $t > t^*$. We also stress here that Eq. 2 has been derived considering the interference effects due to monodisperse hard spheres; in our case this is verified since reduced standard deviation of R_{HS} assumes sufficiently small values as the reaction takes place and goes on. Finally, we note that at $t\approx170$s our main interference peak falls outside the measured *q* range; anyway the higher order maxima and minima falling in our range, joint to the use of constrains setting a lower limit for R_{HS} values, allow us to yield converging fits of experimental data with *rds* of R_{HS} and η that remain less than 0.1, as shown in Fig. 2.

In Fig. 3 we show the $I_B(q)$ and $I_P(q)$ obtained from the optimization procedure, while all different contributions in the model (Eq. 2) are reported in the Fig. 4, where also the log-normal size distributions at two different time intervals are illustrated.

Figures:

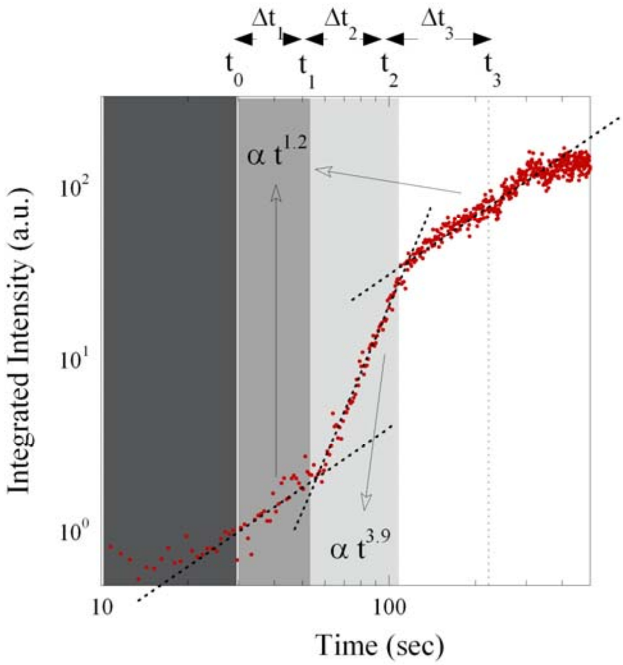

Figure 1: Log-Log plot of integrated intensity vs. time; different power law behaviours (continuous lines) characterize the different time regions $\Delta t_1=[t_1-t_0]$, $\Delta t_2=[t_2-t_1]$ and $\Delta t_3=[t_3-t_2]$.

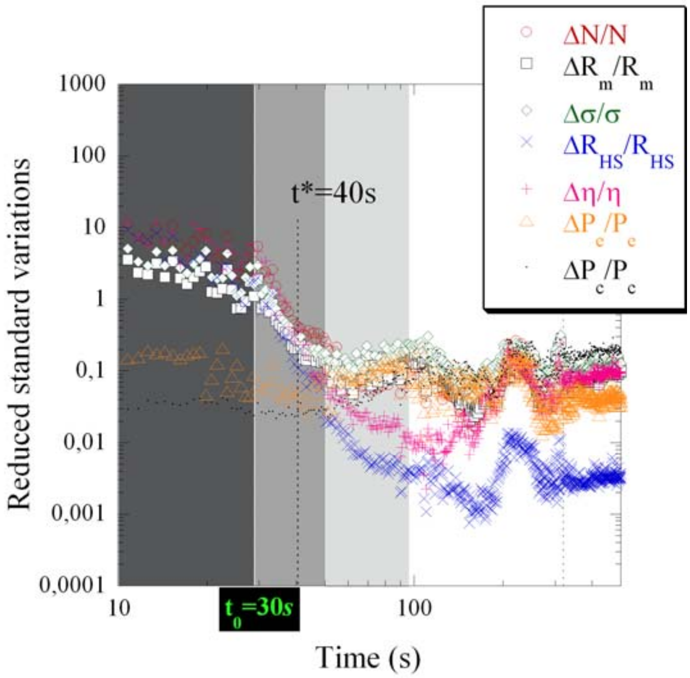

Figure 2: Plot of reduced standard deviations, *rds*, of variable parameters in the fitting procedure; for $t<t^*$, we find large uncertainties of N, R_m, σ, R_{HS}, and η variable parameters, meaning the failure of Eq. 2 in modelling experimental data; here the only power law term of Eq 2 gives small *rds* $\Delta P_E/P_E$ and $\Delta P_C/P_C$. After t^*, the *rds* oscillate around reasonable small values.

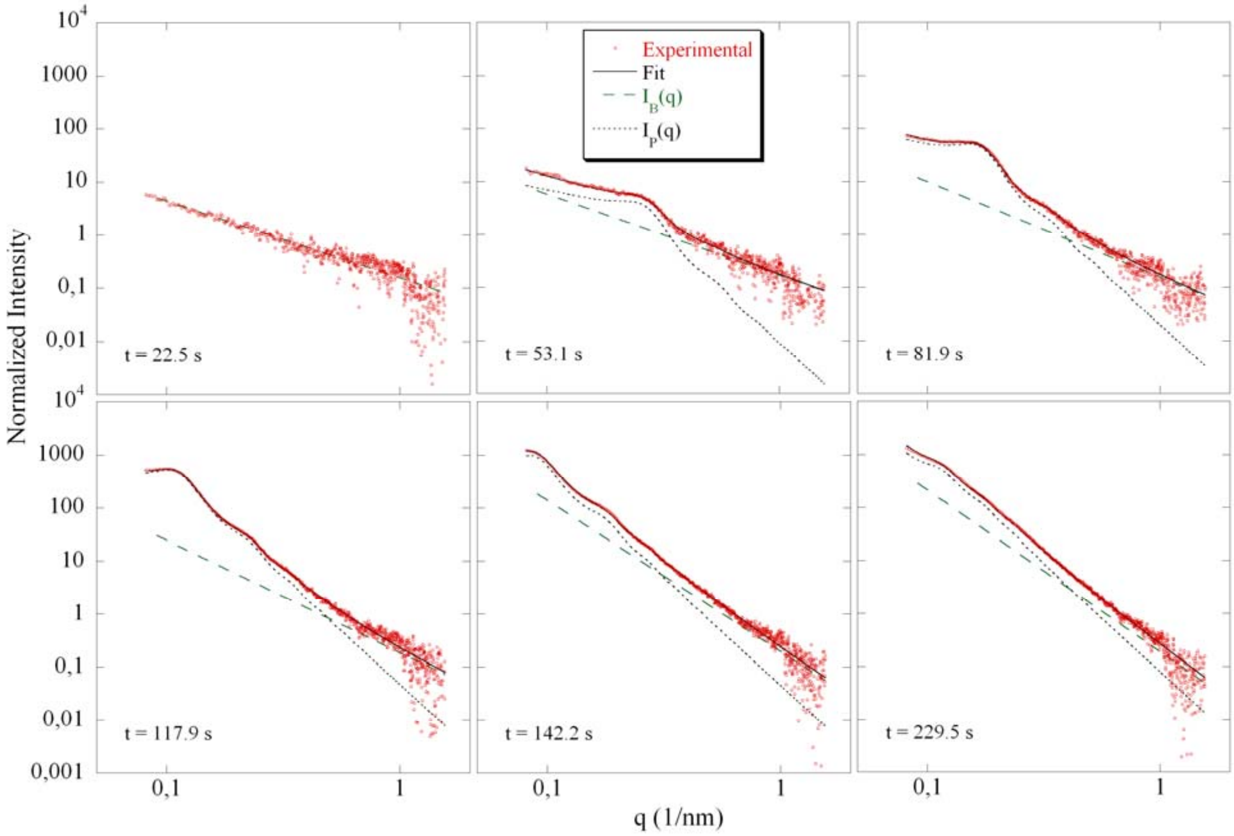

Figure 3: SAXS normalized profiles (dots) collected at the time intervals indicated; solid lines show the best-fitted curves obtained by Eq. 2, while dashed and dotted lines represent the calculated $I_B(q)$ and $I_P(q)$ respectively.

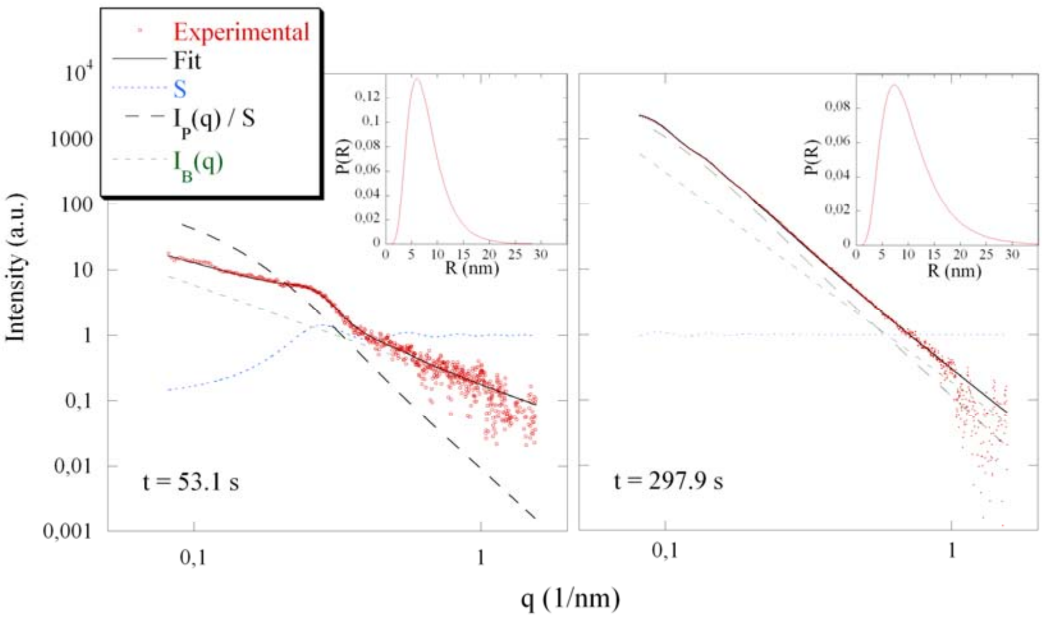

Figure 4: SAXS experimental profiles (red dots) collected at the time intervals indicated along the best-fitted curves solid lines) obtained by Eq. 1.We also represent: the Percus-Yevick structure factor, the power law contribution $I_B(q)$ and the integral $I_P(q)/S = Cn\int_0^\infty P(R)\left[V(R)\Phi(q,R)\right]^2 dR$. The log-normal size distributions, are reported in the insets.